Velocity-gradient probability distribution functions in a lagrangian model of turbulence

J. Stat. Mech. (2014) P10015

(http://iopscience.iop.org/1742-5468/2014/10/P10015)

Journal of Statistical Mechanics: Theory and Experiment
An IOP and SISSA journal

Velocity-gradient probability distribution functions in a lagrangian model of turbulence

L Moriconi[1], R M Pereira[2,3] and L S Grigorio[4]

[1] Instituto de Física, Universidade Federal do Rio de Janeiro, C.P. 68528, CEP: 21945-970, Rio de Janeiro, RJ, Brazil
[2] Laboratoire de Physique, École Normale Supérieure de Lyon, 46 Allée d'Italie, F-69364 Lyon cedex 7, France
[3] Instituto Nacional de Metrologia, Normalização e Qualidade Industrial, Av. Nossa Senhora das Graças 50, Duque de Caxias, RJ 25250-020, Brazil
[4] Centro Federal de Educação Tecnológica Celso Suckow da Fonseca, Av. Governador Roberto Silveira 1900, Nova Friburgo, 28635-000, Brazil
E-mail: rodrigo.pereira@ens-lyon.fr

Received 20 May 2014
Accepted for publication 26 August 2014
Published 9 October 2014

Online at stacks.iop.org/JSTAT/2014/P10015
doi:10.1088/1742-5468/2014/10/P10015

Abstract. The Recent Fluid Deformation Closure (RFDC) model of lagrangian turbulence is recast in path-integral language within the framework of the Martin–Siggia–Rose functional formalism. In order to derive analytical expressions for the velocity-gradient probability distribution functions (vgPDFs), we carry out noise renormalization in the low-frequency regime and find approximate extrema for the Martin–Siggia–Rose effective action. We verify, with the help of Monte Carlo simulations, that the vgPDFs so obtained yield a close description of the single-point statistical features implied by the original RFDC stochastic differential equations.

Keywords: intermittency, lagrangian dynamics, turbulence, stochastic processes (theory)

ArXiv ePrint: 1401.0678

 1742-5468/14/P10015+16$33.00

Contents

1. Introduction

It has long been known, since the seminal work of Batchelor and Townsend [1], that spatial derivatives of a turbulent velocity field do not behave as gaussian random variables. The current view on this still barely understood phenomenon is that the non-gaussian fluctuations of the velocity gradients—the hallmark of turbulent intermittency—are likely to be related to the existence of long-lived coherent structures and to deviations from the Kolmogorov 'K41' scaling, both important ingredients in the contemporary phenomenology of turbulence [2, 3].

The main notorious difficulties with first-principle theories of intermittency stand on (i) the inadequacy of perturbative expansions to deal with the coupled dynamics of vorticity and the rate-of-strain tensor at high Reynolds numbers and (ii) the fact that the closed equations for the time evolution of the velocity gradient tensor are non-local in the space variables. Notwithstanding the strong coupling/non-local issues, it is actually possible to devise simplified fluid dynamical models that would capture relevant qualitative features of the intermittent fluctuations of the velocity gradient tensor [4]. Here, a fundamental role is played by the lagrangian framework of fluid dynamics, since it leads in a natural way to reduced-dimensional systems, in the form of either ordinary or stochastic differential equations for the time evolution of the velocity gradient tensor [5–8].

The aforementioned lagrangian models have mostly been investigated by means of numerical integrations of the associated differential equations, which can then be compared to well-established results of alternative direct numerical simulations. There is however, much room for the exploration of analytical tools in the study of lagrangian models of intermittency, a direction we pursue here, joining other authors in this effort [7,9]. We focus our attention on one particularly interesting stochastic model, the Recent Fluid Deformation Closure (RFDC) model [8] and derive reasonable approximations for its velocity gradient probability distribution functions (vgPDFs). We put into practice standard statistical field-theoretical procedures for the computation of effective actions through vertex renormalization [10–12], which are carried out in the context of the Martin–Siggia–Rose functional formalism [13–16]. Our approach—essentially a semiclassical treatment—is general enough, so that, in principle, it can be applied to a large class of stochastic models.

This paper is organized as follows. In section 2, we briefly outline, as grounds for the subsequent discussions, the essential points of the RFDC model. In section 3, we rephrase the RFDC model in the Martin–Siggia–Rose path-integral formalism and study it through the effective action method. Analytical expressions for the vgPDFs are then obtained. In section 4, we compare, using Monte-Carlo simulations, our vgPDFs with the ones derived from the numerical integration of the RFDC differential stochastic equations. Finally, in section 5, we summarize our main findings and highlight the direction of further research.

J. Stat. Mech. (2014) P10015

2. The RFDC lagrangian stochastic model

Our central object of interest is the time-dependent lagrangian velocity gradient tensor $\mathbb{A}(t)$, which has cartesian components $A_{ij} = \partial_j v_i$. Taking, as a starting point, the Navier-Stokes equations with external gaussian stochastic forcing, the exact lagrangian evolution equation for $\mathbb{A}(t) = \mathbb{A}(\vec{r}(t), t)$ is

$$\dot{\mathbb{A}} = V[\mathbb{A}] + g\mathbb{F}, \tag{1}$$

where $V[\mathbb{A}]$ is a functional of $\mathbb{A}$, defined as

$$V_{ij}[\mathbb{A}] = -(\mathbb{A}^2)_{ij} + \partial_i\partial_j\nabla^{-2}\mathrm{Tr}(\mathbb{A}^2) + \nu\nabla^2(\mathbb{A})_{ij}, \tag{2}$$

and $\mathbb{F}$ is a zero-mean, second order gaussian random tensor, which satisfies

$$\langle F_{ij}(t)F_{kl}(t')\rangle = G_{ijkl}\delta(t-t'), \tag{3}$$

with

$$G_{ijkl} = 2\delta_{ik}\delta_{jl} - \frac{1}{2}\delta_{il}\delta_{jk} - \frac{1}{2}\delta_{ij}\delta_{kl}. \tag{4}$$

Note that there is a space convolution integral in (2), which renders (1) not only non-linear, but non-local as well. Spatial derivatives here are taken with respect to the Eulerian space coordinate and then evaluated along the lagrangian trajectory. In (1), g is just an arbitrary coupling constant proportional to the external power per unit mass, which has an important role in our discussion, since it will be taken as an expansion parameter around the linearized model.

The second and third contributions to the right hand side of (2) are, respectively, the pressure Hessian (written as a non-local functional of the velocity gradient tensor) and the viscous dissipation term. As it stands, (2) is of course not closed: exact solutions on a single lagrangian trajectory are clearly dependent on the bulk space-time profiles of the velocity gradient tensor. However, motivated by the fact that $\mathbb{A}(t)$ is typically short-time correlated, it is natural to conclude that both the pressure Hessian and the viscous dissipation term are dominated by local contributions. This is the point of view taken in the RFDC model of Chevillard and Meneveau [8], where these local contributions are related to the Kolmogorov and the large eddy time scales of the flow, τ and T, respectively (the Reynolds number is, thus, $R_e \propto (T/\tau)^2$). It is then assumed that the lagrangian evolution of $\mathbb{A}(t)$ is associated, for small time scales, to the approximate Cauchy-Green tensor

$$\mathbb{C} = \exp[\tau\mathbb{A}]\exp[\tau\mathbb{A}^{\mathrm{T}}], \tag{5}$$

so that the functional $V[\mathbb{A}]$ in (1) gets replaced by a local function of $\mathbb{A}$,

$$V(\mathbb{A}) = -\mathbb{A}^2 + \frac{\mathbb{C}^{-1}\mathrm{Tr}(\mathbb{A}^2)}{\mathrm{Tr}(\mathbb{C}^{-1})} - \frac{\mathrm{Tr}(\mathbb{C}^{-1})}{3T}\mathbb{A}. \tag{6}$$

We end up, therefore, with a closed and much simpler time evolution equation for $\mathbb{A}$:

$$\dot{\mathbb{A}} = V(\mathbb{A}) + g\mathbb{F} = -\mathbb{A}^2 + \frac{\mathbb{C}^{-1}\mathrm{Tr}(\mathbb{A}^2)}{\mathrm{Tr}(\mathbb{C}^{-1})} - \frac{\mathrm{Tr}(\mathbb{C}^{-1})}{3T}\mathbb{A} + g\mathbb{F}. \tag{7}$$

We refer the reader to [8] for a more detailed account on the conceptual and technical aspects of the RFDC model.

It is convenient to set $T = 1$ (without loss of generality) and perform an expansion of $V(\mathbb{A})$ up to some arbitrary power of τ in (6). A previous extensive numerical study shows that even the first order expansion is enough to grasp the physical content of the model [17]. We work, throughout the paper, with second order expansions of $V(\mathbb{A})$, which we write as

$$V(\mathbb{A}) = \sum_{p=1}^{4} V_p(\mathbb{A}), \tag{8}$$

where

$$V_1(\mathbb{A}) = -\mathbb{A}, \tag{9}$$

$$V_2(\mathbb{A}) = -\mathbb{A}^2 + \frac{\mathbb{I}}{3}\mathrm{Tr}(\mathbb{A}^2) + \frac{2\tau}{3}\mathrm{Tr}(\mathbb{A})\mathbb{A}, \tag{10}$$

$$\begin{aligned} V_3(\mathbb{A}) = & -\frac{\tau}{3}\left(\mathbb{A} + \mathbb{A}^{\mathrm{T}} - \frac{2\mathbb{I}}{3}\mathrm{Tr}(\mathbb{A})\right)\mathrm{Tr}(\mathbb{A}^2) - \frac{\tau^2}{3}\mathrm{Tr}(\mathbb{A}^{\mathrm{T}}\mathbb{A})\mathbb{A} \\ & -\frac{\tau^2}{3}\mathrm{Tr}(\mathbb{A}^2)\mathbb{A}, \end{aligned} \tag{11}$$

$$\begin{aligned} V_4(\mathbb{A}) = & -\frac{\mathbb{I}}{9}\tau^2\mathrm{Tr}(\mathbb{A}^{\mathrm{T}}\mathbb{A})\mathrm{Tr}(\mathbb{A}^2) - \frac{\mathbb{I}}{9}\tau^2[\mathrm{Tr}(\mathbb{A}^2)]^2 + \frac{4\mathbb{I}}{27}\tau^2[\mathrm{Tr}(\mathbb{A})]^2\mathrm{Tr}(\mathbb{A}^2) \\ & + \frac{\tau^2}{3}\mathbb{A}^{\mathrm{T}}\mathbb{A}\mathrm{Tr}(\mathbb{A}^2) + \frac{\tau^2}{6}(\mathbb{A}^2 + \mathbb{A}^{\mathrm{T}}T)\mathrm{Tr}(\mathbb{A}^2). \end{aligned} \tag{12}$$

Thus, it is clear that $V_p(\mathbb{A})$ comprises all the contributions of $O(\mathbb{A}^p)$ to $V(\mathbb{A})$. Note that there is no dimensional inconsistency in the above expansions, since the velocity gradient tensor has a dimension of inverse of time and T has been taken to be the time measurement standard by definition (that is, $T = 1$), so that T is actually hidden (with no loss of physical content) in the power series expansion (8). The RFDC model yields a promising stage for further improvements, insofar as its vgPDFs as well as its geometrical statistical properties related to the coupling between the vorticity and the rate-of-strain tensor share several qualitative features in common with the ones observed in experiments and direct numerical simulations of turbulence [18, 19].

3. Path-integral formulation of the RFDC model

Assume that at time $t_0 = 0$ the velocity gradient tensor is $\mathbb{A}(0) \equiv \mathbb{A}_0$. We may write, within the framework of the Martin–Siggia–Rose (MSR) functional formalism [13–16], the following path-integral expression for the conditional probability density function of finding, at time $t_1 = \beta$, the velocity gradient tensor $\mathbb{A}(\beta) \equiv \mathbb{A}_1$,

$$\rho(\mathbb{A}_1|\mathbb{A}_0, \beta) \equiv \mathcal{N} \int_\Sigma D[\hat{\mathbb{A}}]D[\mathbb{A}] \exp\left\{-S[\hat{\mathbb{A}}, \mathbb{A}]\right\}, \tag{13}$$

where $\mathcal{N}$ is an unimportant normalization factor (which, for convenience, is suppressed from now on),

$$S[\hat{\mathbb{A}}, \mathbb{A}] = \int_0^\beta \mathrm{d}t \left\{ \mathrm{iTr}[\hat{\mathbb{A}}^{\mathrm{T}} L(\mathbb{A})] + \frac{g^2}{2} G_{ijkl} \hat{A}_{ij} \hat{A}_{kl} \right\} \tag{14}$$

with

$$L(\mathbb{A}) \equiv \dot{\mathbb{A}} - V(\mathbb{A}) \tag{15}$$

is the so-called MSR action and

$$\Sigma = \{\mathbb{A}(0) = \mathbb{A}_0,\ \mathbb{A}(\beta) = \mathbb{A}_1\} \tag{16}$$

specifies the set of boundary conditions in the path integration. In the above expressions, $\hat{\mathbb{A}} = \hat{\mathbb{A}}(t)$ is an auxiliary tensor field (a time-dependent 3×3 matrix) with no direct physical meaning. The conditional PDF given in (13) is nothing but a formal solution, written with path-integral dressing of the Fokker-Planck equation that can be derived from the stochastic differential equation (7).

3.1. General strategy for the derivation of vgPDFs

Taking $\beta \to \infty$ in the conditional PDF (13), we obtain the stationary vgPDF evaluated at $\mathbb{A}_1$, which is expected to be independent from the initial condition $\mathbb{A}_0$. Also, as is clear from the original RFDC equations, in the limit of small g, nonlinear perturbations become negligible and all we get are gaussian distributions for the vgPDFs. Thus, we are interested in investigating how the vgPDFs evolve as the noise strength g gets progressively larger and intermittency effects cannot be neglected any more.

Once the conditional vgPDF (13) is independent upon the initial condition $\mathbb{A}_0$, for $\beta \to \infty$, we may impose the particular periodic boundary conditions

$$\mathbb{A}(0) = \mathbb{A}(\beta) = \bar{\mathbb{A}}, \tag{17}$$

J. Stat. Mech. (2014) P10015

motivated by the assumption (verified in numerical studies) that there is no singular behaviour in the time evolution of velocity gradients, as predicted by the RFDC model. The choice of periodic boundary conditions for $\mathbb{A}(t)$ is in fact very convenient, since, as we will see, it leads to considerable computational simplifications. The probability density function of having $\mathbb{A}(t) = \bar{\mathbb{A}}$ at an arbitrary time instant t in the asymptotic stationary fluctuation regime is given, therefore, by

$$\rho(\bar{\mathbb{A}}) = \lim_{\beta \to \infty} \rho(\bar{\mathbb{A}}|\bar{\mathbb{A}}, \beta). \tag{18}$$

We adopt, in our treatment, the path-integral semiclassical approach [10–12], which is a suitable framework to deal with the outset of strong coupling regimes. The whole analysis is based on the existence of dominant configurations $\hat{\mathbb{A}}^{sp}$ and $\mathbb{A}^{sp}$ that satisfy the saddle-point equations

$$\left.\frac{\delta S[\hat{\mathbb{A}}^{sp}, \mathbb{A}]}{\delta A_{ij}}\right|_{\mathbb{A}=\mathbb{A}^{sp}} = 0, \tag{19}$$

$$\left.\frac{\delta S[\hat{\mathbb{A}}, \mathbb{A}^{sp}]}{\delta \hat{A}_{ij}}\right|_{\hat{\mathbb{A}}=\hat{\mathbb{A}}^{sp}} = 0, \tag{20}$$

subject to the boundary conditions $\mathbb{A}^{sp}(0) = \mathbb{A}^{sp}(\beta) = \bar{\mathbb{A}}$. The MSR action can then be expanded, up to the second order, around its saddle-point solutions, through the substitutions $\hat{\mathbb{A}} \to \hat{\mathbb{A}}^{sp} + \hat{\mathbb{A}}$ and $\mathbb{A} \to \mathbb{A}^{sp} + \mathbb{A}$ in (14), viz.,

$$S[\hat{\mathbb{A}}, \mathbb{A}] \to S[\hat{\mathbb{A}}, \mathbb{A}] = S[\hat{\mathbb{A}}^{sp}, \mathbb{A}^{sp}] + \Delta S[\hat{\mathbb{A}}, \mathbb{A}], \tag{21}$$

where $\Delta S[\hat{\mathbb{A}}, \mathbb{A}]$ is a quadratic functional of $\hat{\mathbb{A}}$ and $\mathbb{A}$. We have, accordingly,

$$\rho(\bar{\mathbb{A}}) = \exp\left\{-S[\hat{\mathbb{A}}^{sp}, \mathbb{A}^{sp}]\right\} \int D[\hat{\mathbb{A}}] D[\mathbb{A}] \exp\left\{-\Delta S[\hat{\mathbb{A}}, \mathbb{A}]\right\}. \tag{22}$$

The path-integration over fluctuations in (22) can be computed, within the lowest order in perturbation theory, along the following straightforward two-step procedure:

Step 1. Decompose $\Delta S[\hat{\mathbb{A}}, \mathbb{A}]$ in two terms,

$$\Delta S[\hat{\mathbb{A}}, \mathbb{A}] = \Delta S_0[\hat{\mathbb{A}}, \mathbb{A}] + \Delta S_1[\hat{\mathbb{A}}, \mathbb{A}], \tag{23}$$

where $\Delta S_0[\hat{\mathbb{A}}, \mathbb{A}]$ is quadratic and independent on the saddle-point solutions. More explicitly,

$$\Delta S_0[\hat{\mathbb{A}}, \mathbb{A}] = \int_0^\beta \mathrm{d}t \left\{ \mathrm{i}\mathrm{Tr}[\hat{\mathbb{A}}^{\mathrm{T}}(\dot{\mathbb{A}} - \mathbb{A})] + \frac{g^2}{2} G_{ijkl} \hat{A}_{ij} \hat{A}_{kl} \right\}. \tag{24}$$

There is, on the other hand, a large number of saddle-point dependent contributions in the definition of $\Delta S_1[\hat{\mathbb{A}}, \mathbb{A}]$. As a simplifying working hypothesis, we retain only one of these terms, which leads to meaningful comparisons with the empirical vgPDFs. The truncation is given as

$$\Delta S_1[\hat{\mathbb{A}}, \mathbb{A}] = \mathrm{i} \int_0^\beta \mathrm{d}t \mathrm{Tr}[(\hat{\mathbb{A}}^{sp})^{\mathrm{T}} V_2(\mathbb{A})]. \tag{25}$$

J. Stat. Mech. (2014) P10015

As will become more clear very soon, the physical mechanism behind (25) is such that fluctuations produce, as a main effect, an enhancement of the external random forcing, while not modifying the original structure of the non-linear response in the RFDC model, well captured by the corresponding terms of the MSR saddle-point action.

Step 2. Within the lowest non-trivial order of perturbation theory, apply the standard second-order cumulant expansion, in the present context, to get

$$\int D[\hat{\mathbb{A}}]D[\mathbb{A}] \exp\left\{-\mathit{\Delta} S[\hat{\mathbb{A}},\mathbb{A}]\right\}$$
$$= \int D[\hat{\mathbb{A}}]D[\mathbb{A}] \exp\left\{-\mathit{\Delta} S_0[\hat{\mathbb{A}},\mathbb{A}] - \mathit{\Delta} S_1[\hat{\mathbb{A}},\mathbb{A}]\right\}$$
$$= \exp\left[\frac{1}{2}\langle(\mathit{\Delta} S_1[\hat{\mathbb{A}},\mathbb{A}])^2\rangle_0\right], \quad (26)$$

where $\langle(...)\rangle_0$ stands for the expectation value computed in the model defined by the quadratic action $\mathit{\Delta} S_0[\hat{\mathbb{A}},\mathbb{A}]$. In order to derive (26), we have taken into account that $\langle \mathit{\Delta} S_1[\hat{\mathbb{A}},\mathbb{A}]\rangle_0 = 0$, as it is found in a detailed calculation. Using (26), equation (22) is replaced, therefore, by the improved vgPDF

$$\rho(\bar{\mathbb{A}}) = \exp\left\{-\mathit{\Gamma}[\hat{\mathbb{A}}^{sp},\mathbb{A}^{sp}]\right\}, \quad (27)$$

where

$$\mathit{\Gamma}[\hat{\mathbb{A}}^{sp},\mathbb{A}^{sp}] \equiv S[\hat{\mathbb{A}}^{sp},\mathbb{A}^{sp}] - \frac{1}{2}\langle(\mathit{\Delta} S_1[\hat{\mathbb{A}},\mathbb{A}])^2\rangle_0 \quad (28)$$

is referred to as the 'MSR Effective Action'. It is important to note that the effective action $\mathit{\Gamma}[\hat{\mathbb{A}},\mathbb{A}]$ satisfies, within the lowest order of perturbation theory, saddle-point equations analogous to those given in (19) and (20). Without affecting the accuracy of the results, one can postpone—as we will—the derivation of saddle-point configurations to the stage where the form of the effective action has been already established.

3.2. Structure of the MSR effective action

The truncated form (25) for the saddle-point dependent quadratic fluctuations leads to noise renormalization, which amounts to saying that the operator kernel $G_{ijkl}\delta(t-t')$ in (13) is substituted by an alternative one, $G^{\mathrm{ren}}_{ijkl}(t-t')$, so that the MSR effective action becomes

$$\mathit{\Gamma}[\hat{\mathbb{A}},\mathbb{A}] = i\int_0^\beta \mathrm{d}t \mathrm{Tr}[\hat{\mathbb{A}}^{\mathrm{T}} L(\mathbb{A})] + \frac{g^2}{2}\int_0^\beta \mathrm{d}t \int_0^\beta \mathrm{d}t' G^{\mathrm{ren}}_{ijkl}(t-t')\hat{A}_{ij}(t)\hat{A}_{kl}(t'). \quad (29)$$

As is usually done in effective action studies [10–12], we work with low-frequency renormalization. This procedure consists in the replacement of the operator kernel $G^{\mathrm{ren}}_{ijkl}(t-t')$ by $\tilde{G}^{\mathrm{ren}}_{ijkl}\delta(t-t')$, where

$$\tilde{G}^{\mathrm{ren}}_{ijkl} \equiv \int_{-\infty}^{\infty} \mathrm{d}t G^{\mathrm{ren}}_{ijkl}(t). \quad (30)$$

Low-frequency renormalization is actually a welcome simplification in several relevant instances such as (i) in the evaluation of the translationally invariant ground state

J. Stat. Mech. (2014) P10015

expectation values of observables of interest, (ii) in renormalization group studies near the vicinity of second order phase transitions (since the order parameter fluctuations are long-ranged) and (iii) in dynamical regimes characterised by the presence of solitons/instantons defined on a large enough space or time scale [20]. In our particular case, even if we do not have a strong separation of scales (Reynolds numbers are not very high), we are motivated by the fact that the saddle-point solutions, as we will see, have characteristic time scales of the order of $T(=1)$, which is the largest time scale of the RFDC model.

Taking into account now, as the result of calculations, that $G^{\rm ren}_{iikl} = G^{\rm ren}_{ijkk} = 0$, we may introduce the x and y parameters to define

$$\tilde{G}^{\rm ren}_{ijkl} \equiv D_{ijkl} - \frac{1}{3}(x+y)\delta_{ij}\delta_{kl}, \tag{31}$$

where

$$D_{ijkl} \equiv x\delta_{ik}\delta_{jl} + y\delta_{il}\delta_{jk}. \tag{32}$$

Furthermore it is not difficult to show, from the saddle-point equations for the effective action, that the latter may be written as a functional of the velocity gradient tensor $\mathbb{A}$, which makes no reference to the auxiliary field $\hat{\mathbb{A}}$:

$$\varGamma[\mathbb{A}] = \frac{1}{2g^2}\int_0^\beta {\rm d}t \left[D^{-1}_{ijkl}L_{ij}(\mathbb{A})L_{kl}(\mathbb{A})\right], \tag{33}$$

where D^{-1}_{ijkl} is the tensor inverse of D_{ijkl},

$$D^{-1}_{ijkl} \equiv a\delta_{ik}\delta_{jl} + b\delta_{il}\delta_{jk}, \tag{34}$$

with

$$a = -\frac{x}{y^2-x^2}, \;\; b = \frac{y}{y^2-x^2}. \tag{35}$$

We underline that $\mathbb{A}^{sp}$ can be directly obtained from the single saddle-point equation

$$\left.\frac{\delta\varGamma[\mathbb{A}]}{\delta A_{ij}}\right|_{\mathbb{A}=\mathbb{A}^{sp}} = 0, \tag{36}$$

a useful result, as discussed below.

3.3. Saddle-point solutions

It is a difficult—if not actually impossible—task to obtain the exact saddle-point solution of (36). Around the small g regime, however, we can keep only the quadratic terms in the effective action, as a first approximation. From (33) and (34), we find, in the quadratic approximation,

$$\varGamma[\mathbb{A}] \equiv \frac{a}{2g^2}\int_0^\beta {\rm d}t{\rm Tr}\left[\dot{\mathbb{A}}^{\rm T}\dot{\mathbb{A}} + \mathbb{A}^{\rm T}\mathbb{A}\right] + \frac{b}{2g^2}\int_0^\beta {\rm d}t{\rm Tr}\left[\dot{\mathbb{A}}^2 + \mathbb{A}^2\right]. \tag{37}$$

The saddle-point equation (36) yields, in this case,

$$\ddot{\mathbb{A}} - \mathbb{A} = 0. \tag{38}$$

J. Stat. Mech. (2014) P10015

The solution of (38) that satisfies the boundary conditions (17) is

$$\mathbb{A}^{sp}(t) = \bar{\mathbb{A}} f_\beta(t), \tag{39}$$

where

$$f_\beta(t) = 2\frac{\sinh(\frac{\beta}{2})}{\sinh(\beta)} \cosh(t - \frac{\beta}{2}). \tag{40}$$

Substituting, now, (39) in (8), we obtain

$$V(\mathbb{A}^{sp}(t)) = \sum_{p=1}^{4} V_p(\bar{\mathbb{A}})[f_\beta(t)]^p. \tag{41}$$

The MSR effective action is therefore written, in the limit where $\beta \to \infty$, as

$$\Gamma[\mathbb{A}^{sp}] \equiv \Gamma(\bar{\mathbb{A}}) = \Gamma_1(\bar{\mathbb{A}}) + \Gamma_2(\bar{\mathbb{A}}), \tag{42}$$

with

$$\Gamma_1(\bar{\mathbb{A}}) = \frac{a}{2g^2} \mathrm{Tr}\left[I_1 \bar{\mathbb{A}}^{\mathrm{T}} \bar{\mathbb{A}} + \sum_{p=1}^{4}\sum_{q=1}^{4} I_{p+q} V_p(\bar{\mathbb{A}}^{\mathrm{T}}) V_q(\bar{\mathbb{A}}) \right], \tag{43}$$

and

$$\Gamma_2(\bar{\mathbb{A}}) = \frac{b}{2g^2} \mathrm{Tr}\left[I_1 \bar{\mathbb{A}}^2 + \sum_{p=1}^{4}\sum_{q=1}^{4} I_{p+q} V_p(\bar{\mathbb{A}}) V_q(\bar{\mathbb{A}}) \right], \tag{44}$$

where the above I-coefficients are defined as

$$I_1 = \lim_{\beta\to\infty} \int_0^\beta \mathrm{d}t [\dot{f}_\beta(t)]^2, \;\; I_{p+q} = \lim_{\beta\to\infty} \int_0^\beta \mathrm{d}t [f_\beta(t)]^{p+q}. \tag{45}$$

Their numerical values are listed below:

$$\begin{aligned} &I_1 = I_2 = 1, \;\; I_3 = 2/3, \;\; I_4 = 1/2, \\ &I_5 = 2/5, \;\; I_6 = 1/3, \;\; I_7 = 2/7, \;\; I_8 = 1/4. \end{aligned} \tag{46}$$

We emphasize, at this point, that the number of terms that contribute to $\Gamma(\bar{\mathbb{A}})$ would be unnecessarily larger had we not used periodic boundary conditions for $\mathbb{A}^{sp}(t)$. This is because, due to the periodic boundary conditions, the several time integrations of tensorial products involving only one time derivative of the velocity gradient tensor can be completely removed for the evaluation of the effective action.

3.4. Noise renormalization

As we have already seen, in our particular problem the MSR effective action is given by the MSR saddle-point action added to $-\langle(\Delta S_1[\hat{\mathbb{A}}, \mathbb{A}])^2\rangle_0/2$. We have, more concretely,

$$-\frac{1}{2}\langle(\Delta S_1[\hat{\mathbb{A}}, \mathbb{A}])^2\rangle_0 = \frac{1}{2}\int_0^\beta \mathrm{d}t \int_0^\beta \mathrm{d}t' \hat{A}^{sp}_{ij}(t)\hat{A}^{sp}_{kl}(t') C_{ijkl}(t-t'), \tag{47}$$

where

$$C_{ijkl}(t-t') = \langle [V_2(\mathbb{A}(t))]_{ij} [V_2(\mathbb{A}(t'))]_{kl}\rangle_0. \tag{48}$$

J. Stat. Mech. (2014) P10015

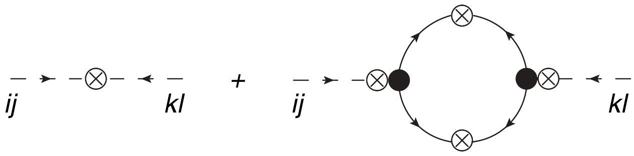

Figure 1. The Feynman diagram contributions to the noise vertex renormalization of the effective Martin–Siggia–Rose action, up to $\mathrm{O}(g^4)$. The free one-particle propagators are represented by directed lines. The bare noise vertices are depicted as isolated crossed circles linked to two convergent lines. The bare three-point vertices are associated to the contributions provided by $V_2(\mathbb{A})$ in the RFDC stochastic time evolution equation (7).

It is clear, from the form of (47), that this contribution renormalizes the noise term as it appears in the original saddle-point MSR action, according to the substitution

$$g^2 G_{ijkl}\delta(t-t') \to g^2 G^{\mathrm{ren}}_{ijkl}(t-t') = g^2 G_{ijkl}\delta(t-t') + C_{ijkl}(t-t'). \tag{49}$$

The two contributions in the right-hand-side of (49) are represented by the two diagrams depicted in figure 1 (a good account on the perturbative diagrammatic expansions for stochastic differential equations can be found in [21]), which use, as graphic elements, the propagator and the noise vertex of the quadratic model given by the action (24).

Recalling, now, the notation introduced in (31) and (32), we find, from the straightforward computation of $C_{ijkl}(t-t')$,

$$x = 2 + \frac{3}{2}g^2, \tag{50}$$

$$y = -\frac{1}{2} - \frac{1}{16}g^2. \tag{51}$$

We determine, from equations (50) and (51), the a and b parameters defined in (35) and use them to conclude the evaluation of the MSR effective action (42), taking into account (43) and (44). The vgPDF can then, be readily written (up to a normalization factor) as $\rho(\bar{\mathbb{A}}) = \exp[-\Gamma(\bar{\mathbb{A}})]$.

In order to estimate what has been missed by the truncation (25), it is interesting to have a deeper look at the structure of the diagrammatic expansion of the MSR effective action. It is not difficult to show that a diagram that contains L loops and E incoming external lines produces a contribution to the effective action which is proportional to $g^{2(L+E-1)}$. The perturbative expansion of the effective action can be hierarchized, therefore, from the number of loops that each one of its diagram's contains. The situation here is entirely analogous to the one long known in usual quantum field theory models (or even in quantum mechanics), where the number of loops in the diagrammatic expansion of the effective action is associated to powers of the Planck constant [12]. Note that the analogy between g^2 and the Planck constant becomes explicit if the auxiliary random variable $\hat{\mathbb{A}}$ is integrated out from the formalism, as in equation (33).

An important additional point to stress is that g is not the only coupling constant to appear in the loop expansion of the effective action for the RFDC model. Powers of the dissipative time scale τ are brought into the one-loop contributions due to the specific form of the vertices V_N defined in (8). In figures 2(a) and (b) we depict the one loop

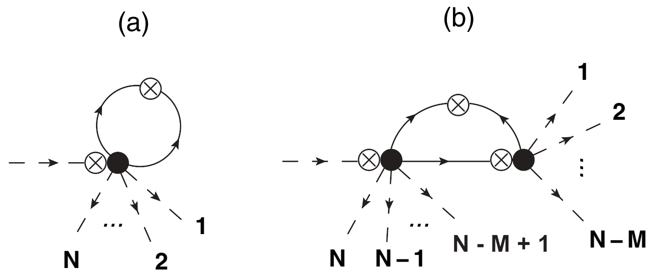

Figure 2. Parts (*a*) and (*b*) show the structure of the one-loop contributions to the vertex renormalization associated to V_N.

diagrams that renormalize the vertex V_N. Note the role, in these diagrams, played by the vertices V_{N+2} (figure 2(*a*)) and V_{N-M+1} and V_{M+2}, with $M < N$ (figure 2(*b*)). In the one-loop renormalization of the vertex V_3, for instance, there is no way to avoid the participation of two vertices V_3 or just one V_4. Both of these contributions are of the order of τ^2. Such 'casual' powers of τ may provide, in fact, a hint as to why the noise is the most important vertex to be corrected at one-loop order: the dynamic regimes of interest have relatively small values of τ [8], so that it is likely that the g^4 correction to the noise vertex, which does not get any power of τ, turns out to be more important than the other vertices corrected with contributions of order τg^2 or $\tau^2 g^2$.

Our approximations were actually motivated by both theoretical expectations and general qualitative features that have emerged from the accumulated numerical experience on the RFDC model, which are described as follows.

(a) It is clear, from (1), that as g becomes small, the velocity gradient fluctuations become small as well, so that the non-linear terms in (1) can be neglected in that limit. Therefore, in the limit of vanishing g, the saddle-point solution given in (39) is exact, the velocity gradient fluctuations are described by gaussian statistics (since the associated Langevin equations are linear) and there would be no need of renormalization.

(b) As previous numerical studies have suggested, the RFDC model provides a meaningful account of intermittency effects only at the outset of turbulent behaviour. This is just another way of saying that the model allows us to study phenomena in the range of low to moderate Reynolds numbers. Therefore, one has necessarily to work in regimes close to the 'gaussian point', which justifies our use of perturbative computations in the analysis of the RFDC model and the substitution of the saddle-point solution in the fully non-linear Martin–Siggia–Rose action (after noise renormalization is taken into account).

(c) It is an empirical (i.e. numerical) result that the shapes of the velocity gradient PDFs are only slightly changed in their cores as higher-order expansions are considered in the expression for $V(\mathbb{A})$, as given by (8)—it would be fine as well to work within the first order expansion in τ. From a purely mathematical perspective, τ is effectively a small parameter and we expect, thus, that the renormalization of the contributions to $V(\mathbb{A})$ which have coefficients proportional to τ would bring only subleading improvements in the analytical form of the velocity gradient PDFs.

(d) It is also an empirical result that the shape of velocity gradient PDFs is very sensitive to variations of the noise strength parameter g. This phenomenon has to do with the

J. Stat. Mech. (2014) P10015

fact that as g increases, larger fluctuations of the velocity gradients will take place and, as a consequence, non-linear terms become more important. This suggests that we focus on noise strength renormalization as the main contribution in the evaluation of the Martin–Siggia–Rose effective action.

4. Analytical versus empirical vgPDFs

Plots of the analytical vgPDFs $\rho(\bar{\mathbb{A}}) \propto \exp[-\Gamma(\bar{\mathbb{A}})]$ can be compared to the empirical PDFs obtained through the direct numerical solutions of the stochastic differential equation (7). We have produced, using the analytical vgPDFs, large Monte Carlo ensembles of velocity gradients. The numerical solution of (7), on the other hand is carried out within a second order predictor-corrector method [22], with time step $\epsilon = 0.01$. We have considered, in all our numerical tests, $\tau = 0.1$, a reference time-scale usually taken in studies of the RFDC model.

In our Monte Carlo procedure, the velocity gradient $\mathbb{A}$ is additively perturbed by random traceless 3×3 matrices at each iteration step. The stochastic increments can always be written as a linear superposition of matrices of the overcomplete set $\{\mathbb{B}_1, \mathbb{B}_2, ..., \mathbb{B}_9\}$, where

$$\begin{aligned}
\mathbb{B}_1 &= \begin{bmatrix} 0 & 0 & 0 \\ 0 & 0 & 1 \\ 0 & -1 & 0 \end{bmatrix}, \ \mathbb{B}_4 = \begin{bmatrix} 0 & 1 & 0 \\ 1 & 0 & 0 \\ 0 & 0 & 0 \end{bmatrix}, \ \mathbb{B}_7 = \begin{bmatrix} 1 & 0 & 0 \\ 0 & -\frac{1}{2} & 0 \\ 0 & 0 & -\frac{1}{2} \end{bmatrix}, \\
\mathbb{B}_2 &= \begin{bmatrix} 0 & 0 & 1 \\ 0 & 0 & 0 \\ -1 & 0 & 0 \end{bmatrix}, \ \mathbb{B}_5 = \begin{bmatrix} 0 & 0 & 0 \\ 0 & 0 & 1 \\ 0 & 1 & 0 \end{bmatrix}, \ \mathbb{B}_8 = \begin{bmatrix} -\frac{1}{2} & 0 & 0 \\ 0 & 1 & 0 \\ 0 & 0 & -\frac{1}{2} \end{bmatrix}, \\
\mathbb{B}_3 &= \begin{bmatrix} 0 & 1 & 0 \\ -1 & 0 & 0 \\ 0 & 0 & 0 \end{bmatrix}, \ \mathbb{B}_6 = \begin{bmatrix} 0 & 0 & 1 \\ 0 & 0 & 0 \\ 1 & 0 & 0 \end{bmatrix}, \ \mathbb{B}_9 = \begin{bmatrix} -\frac{1}{2} & 0 & 0 \\ 0 & -\frac{1}{2} & 0 \\ 0 & 0 & 1 \end{bmatrix}.
\end{aligned} \tag{52}$$

Observe that the above matrices are special generators of three-dimensional rotations $(\mathbb{B}_1, \mathbb{B}_2, \mathbb{B}_3)$, reflections $(\mathbb{B}_4, \mathbb{B}_5, \mathbb{B}_6)$ and shearing transformations $(\mathbb{B}_7, \mathbb{B}_8, \mathbb{B}_9)$. In more precise terms, the ensemble of velocity gradients is produced from successive stochastic perturbations of $\mathbb{A}$ given as

$$\mathbb{A} \to \mathbb{A}' = \mathbb{A} + s\mathbb{B}_p. \tag{53}$$

Let $\Delta\Gamma(s) \equiv \Gamma(\mathbb{A}') - \Gamma(\mathbb{A})$ and χ be a gaussian random variable which is sorted at each Monte Carlo step, with zero mean and some standard deviation σ, to be defined below. In order to set s in (53), the Metropolis algorithm [23] is then applied as follows:

(a) If $\Delta\Gamma(\chi) < 0$, take $s = \chi$, otherwise define $p = \exp[-\Delta\Gamma(\chi)]$ and go to step (b).

(b) Take $s = \chi$ with probability p and $s = 0$ with probability $1 - p$.

As is usually done in an analogous Monte Carlo simulation context [24], the numerical value of the standard deviation parameter σ is adjusted so that the case $s = 0$ is verified in about 50% of the Monte Carlo steps.

J. Stat. Mech. (2014) P10015

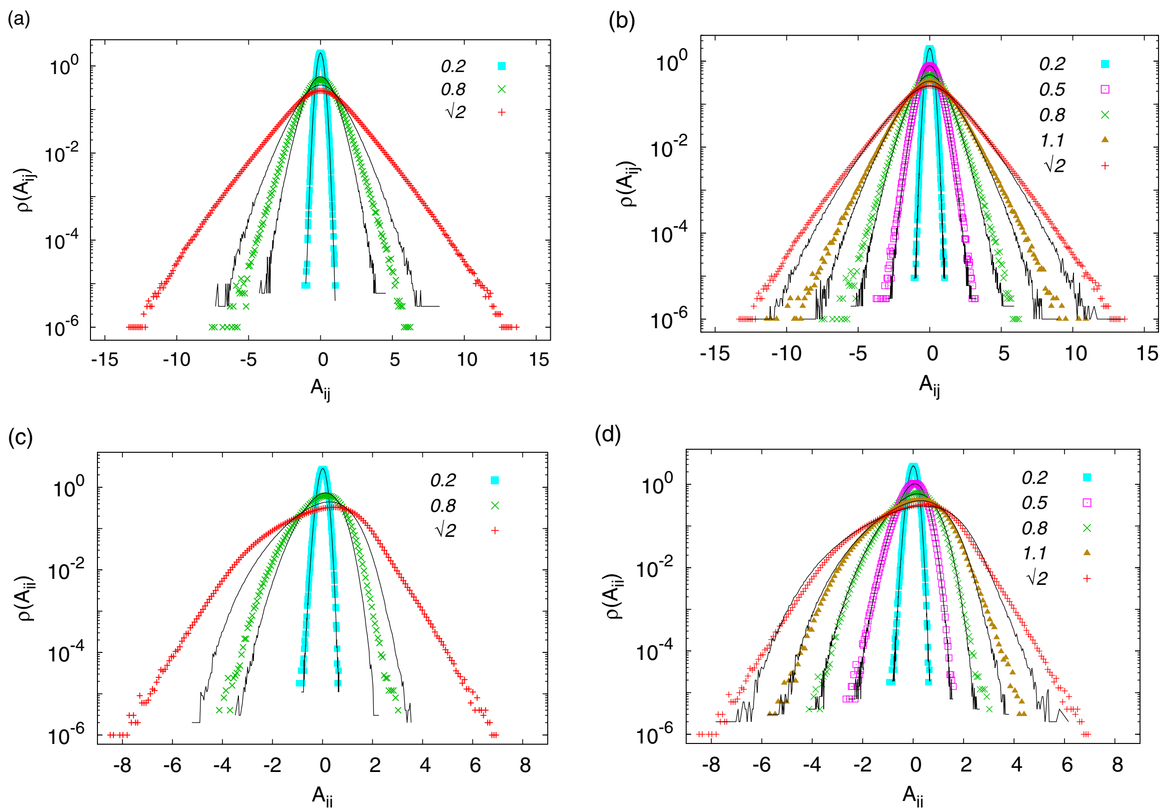

Figure 3. Comparative semi-log plots of vgPDFs. The solid lines represent the analytical vgPDFs evaluated for $\tau = 0.1$ and some values of the bare noise strength g with and without noise renormalization. The vgPDFs depicted with symbols refer to those obtained from the direct numerical integration of the RFDC stochastic equations. The vgPDFs for the non-diagonal components of the velocity gradient tensor are given in parts (a) (nonrenormalized noise for $g = 0.2, 0.8$ and $\sqrt{2}$) and (b) (renormalized noise for $g = 0.2, 0.5, 0.8, 1.1$ and $\sqrt{2}$). The analogous results for the diagonal components are given in figures (c) and (d).

Samples of non-diagonal and diagonal components of the velocity gradient tensor have been grouped into two distinct sets. We refer, thus, to vgPDFs of non-diagonal and diagonal components of $\mathbb{A}$, without specifying any particular cartesian tensor indices. Our statistical evaluations were performed with sets of 12×10^6 and 24×10^6 elements for the diagonal and non-diagonal components, respectively, of the velocity gradient tensor.

Our results are shown in figures 3–5. In order to appreciate the relevance of noise renormalization, we have also depicted how the vgPDFS would look if the noise vertex were not corrected by the loop diagram of figure 1 (these PDFs are given in figures 3 (a, c) and 4(a, c)). The one-loop correction leads, in fact, to much better approximations for the vgPDFs. The results are even more satisfactory to the eye if the vgPDFs are plotted in linear scales (figure 4), since larger deviations from the analytical expressions are found mostly in the far tails of the vgPDFs and are actually associated to small cumulative probabilities.

The analytical velocity gradient PDFs discussed here allow us to address the outset of intermittency in the RFDC model. In fact, all of them have a positive kurtosis excess (a

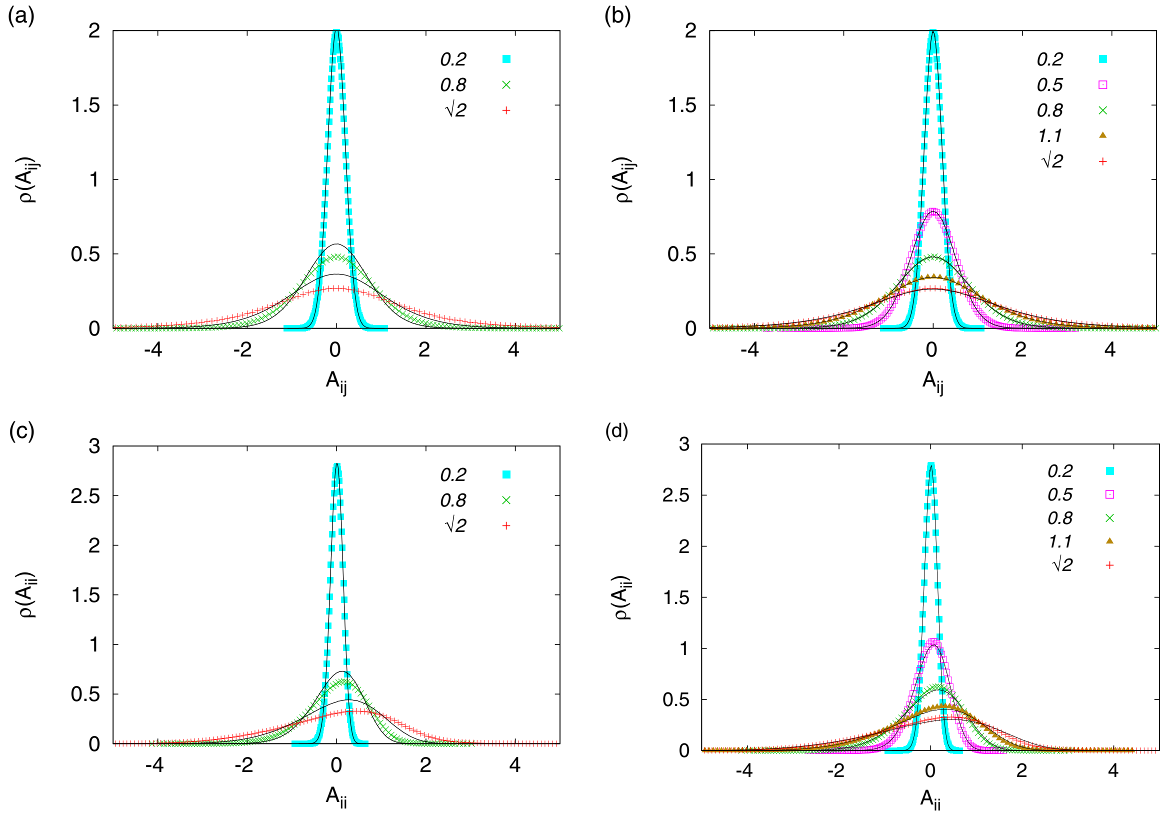

Figure 4. Comparative linear plots of vgPDFs, described in the same way as in figure 3. The fittings in (b) and (d) are very reasonable within about two standard deviations around the peak values of the vgPDFs.

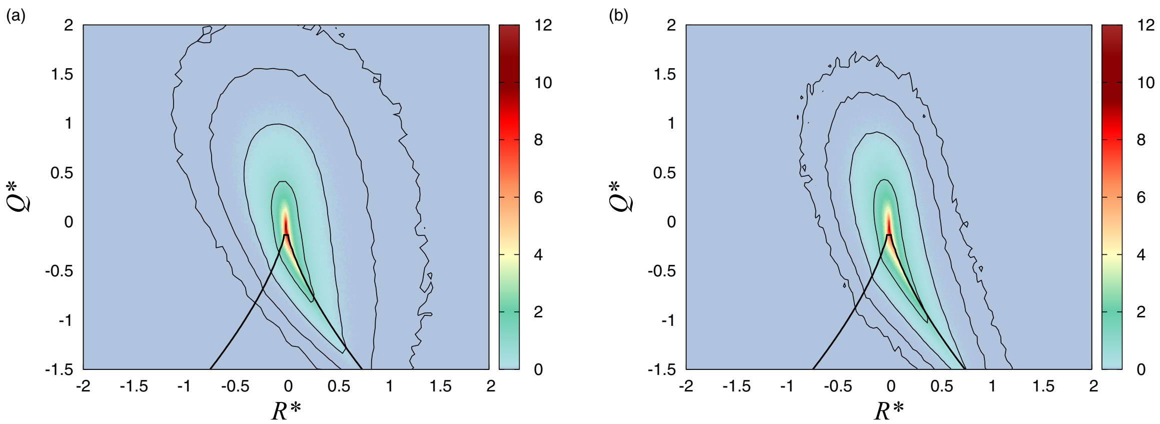

Figure 5. Contour plots for the joint PDFs of the normalized Cayley-Hamilton invariants Q^* and R^* for $\tau = 0.1$ and $g = \sqrt{2}$. The level curves have PDF values equal to 1, 10^{-1}, 10^{-2} and 10^{-3}. Part (a) is obtained from the direct numerical integration of the RFDC stochastic equations, while part (b) is evaluated from the analytical vgPDF discussed in section 3. The inverted V-shaped lines in both parts (a) and (b) indicate the Vieillefosse zero discriminant line.

J. Stat. Mech. (2014) P10015

signature of intermittency) and have their kurtosis reasonably close to the ones associated to the numerical PDFs (maximum error around 10%).

In figure 5 we show how the analytical and the empirical joint probability distributions of the normalized Cayley-Hamilton invariants

$$Q^* = -\frac{\mathrm{Tr}(\mathbb{A}^2)}{2\langle S^2 \rangle} \text{ and } R^* = -\frac{\mathrm{Tr}(\mathbb{A}^3)}{3\langle S^2 \rangle^{3/2}}, \quad (54)$$

where S is the rate-of-strain tensor, with $S^2 \equiv S_{ij}S_{ij}$, compare to each other. We find that the analytical joint PDF accounts for the essential qualitative geometrical features as the 'tear-drop' shapes of the level curves and the role of the zero-discriminant line. The quantitative agreement is better, of course, close to the origin of the (R^*, Q^*) plane, where non-linear fluctuations of the velocity gradient tensor tend to be suppressed.

5. Conclusions

We carried out an analytical study of the vgPDFs in the RFDC lagrangian model of turbulence. The MSR framework in its path-integral formulation proves to be a very convenient setup, where standard field-theoretical semiclassical approaches can be straightforwardly applied. Once it is difficult to establish exact saddle-point solutions for the Euler-Lagrange equations associated either to the bare or to the MSR effective action, we have used, as an approximation, solutions that hold in the regime of small noise strength. A further source of technical difficulty is related to the precise evaluation of the MSR effective action up to one-loop order: in fact, one should take into account a large number of vertex corrections, leading to non-local kernels as the result of much more involved computations. We have, thus, put forward a pragmatic strategy for the evaluation of the MSR effective action where, as working hypotheses, (i) only the noise vertex is corrected up to one-loop order and (ii) a low-frequency approximation for the renormalized noise vertex is implemented. In spite of the above simplifying assumptions, the resulting analytical vgPDFs can be satisfactorily compared to the empirical ones for a meaningful range of bare noise coupling constants ($g < \sqrt{2}$). We leave for additional research the necessary refinements of the approach we have undertaken in this paper. We also note that time-dependent correlation functions of the velocity gradient tensor can be evaluated along similar semiclassical lines.

Analytical vgPDFs are a promising tool in the study of turbulent intermittency. Once validated, they can be used to investigate conditional statistical phenomena in a way that would be not possible through ensembles produced from solutions of the related stochastic differential equations. As a general remark, when one has to hand some analytical expression for the joint probability distribution function of random variables, Monte Carlo procedures can be straightforwardly implemented for the analysis of conditional statistical phenomena. The essential point is to devise Monte Carlo steps that preserve the values of the conditioning quantity. In this way, statistical evaluations related to the conditional pressure Hessian could be devised, a topic of great interest in the subject of lagrangian models of turbulence. Another particularly interesting application of the analytical vgPDFS could be used, in principle, in the context of turbulent geometrical statistics, in order to clarify the statistical relations between the vorticity and the rate-of-strain fields.

As a concluding remark, it is important to emphasize that the semiclassical method approach discussed in this work can be extended, with no further conceptual or technical obstacles, to several turbulence models and to a large class of phase-space reduced stochastic dynamical systems.

Acknowledgments

This work was partially supported by CNPq, CAPES and FAPERJ. LM would like to thank the warm hospitality of the ICTP during the early stages of this work. RMP thanks CAPES for the support through the scholarship process number 9497/13-7. The authors have greatly benefited from the use of NIDF facilities at COPPE-UFRJ.

References

[1] Batchelor G K and Townsend A A 1949 *Proc. R. Soc. Lond.* A **199** 238
[2] Frisch U 1995 *Turbulence: the Legacy of A.N. Kolmogorov* (Cambridge: Cambridge University Press)
[3] Davidson P A 2004 *Turbulence, an Introduction for Scientists and Engineers* (Oxford: Oxford University Press)
[4] Meneveau C 2011 *Ann. Rev. Fluid Mech.* **43** 219
[5] Vieillefosse P 1984 *Physica* A **125** 150
[6] Cantwell B J 1992 *Phys. Fluids* A **4** 782
[7] Chertkov M, Pumir A and Shraiman B I 1999 *Phys. Fluids* **11** 2394
[8] Chevillard L and Meneveau C 2006 *Phys. Rev. Lett.* **97** 174501
[9] Naso A, Pumir A and Chertkov M 2007 *J. Turb.* **8** 1
[10] Amit D 1984 *Field Theory, the Renormalization Group and Critical Phenomena* (Singapore: World Scientific)
[11] Zinn-Justin J J 2002 *Quantum Field Theory and Critical Phenomena* (Oxford: Oxford University Press)
[12] Peskin M E and Schroeder D V 1995 *An Introduction to Quantum Field Theory* (New York: Addison-Wesley)
[13] Martin P C, Siggia E D and Rose H A 1973 *Phys. Rev.* A **8** 423
[14] Janssen H K 1976 *Z. Phys.* B **23** 377
[15] De Dominicis C 1976 *J. Phys. Colloques* **37** C1-247
[16] Cardy J 1996 *Scaling and Renormalization in Statistical Physics* (Cambridge: Cambridge University Press)
[17] Afonso M M and Meneveau C 2010 *Physica* D **239** 1241
[18] Chevillard L and Meneveau C 2011 *Phys. Fluids* **23** 101704
[19] Chevillard L, Meneveau C, Biferale L and Toschi F 2008 *Phys. Fluids* **20** 101504
[20] Rajaraman R 1987 *Solitons and Instantons* (Amsterdam: North-Holland)
[21] Barabasi A-L and Stanley E 1995 *Fractal Concepts in Surface Growth* (Cambridge: Cambridge University Press)
[22] Kloeden P E and Platen E 1999 *Numerical Solution of Stochastic Differential Equations* (Berlin: Springer)
[23] Landau D P and Binder K 2005 *A Guide to Monte Carlo Simulations in Statistical Physics* (Cambridge: Cambridge University Press)
[24] Itzykson C and Drouffe J-M 1991 *Statistical Field Theory* vol 2 (Cambridge: Cambridge University Press)